

Engineering Optimization



ISSN: (Print) (Online) Journal homepage: https://www.tandfonline.com/loi/geno20

Multi-objective optimization for two-dimensional maximum weight lifting prediction considering dynamic strength

Yujiang Xiang, Jazmin Cruz, Rahid Zaman & James Yang

To cite this article: Yujiang Xiang, Jazmin Cruz, Rahid Zaman & James Yang (2021) Multi-objective optimization for two-dimensional maximum weight lifting prediction considering dynamic strength, Engineering Optimization, 53:2, 206-220, DOI: 10.1080/0305215X.2019.1702979

To link to this article: https://doi.org/10.1080/0305215X.2019.1702979

	Published online: 10 Jan 2020.
	Submit your article to this journal 🗷
ılıl	Article views: 250
Q ¹	View related articles ☑
CrossMark	View Crossmark data ☑
4	Citing articles: 2 View citing articles ☑





Multi-objective optimization for two-dimensional maximum weight lifting prediction considering dynamic strength

Yujiang Xiang^a, Jazmin Cruz^b, Rahid Zaman^a and James Yang^b

^aSchool of Mechanical and Aerospace Engineering, Oklahoma State University, Stillwater, OK, USA; ^bHuman-Centric Design Research Lab, Department of Mechanical Engineering, Texas Tech University, Lubbock, TX, USA

ABSTRACT

Manual material handling is common in daily life and is the main cause of lower back pain. Therefore, it is critical to establish a lifting limit for workers. However, it is difficult to obtain each individual's maximum lifting weight through experiments. This study presents a multi-objective optimization (MOO) for two-dimensional maximum weight lifting prediction. Minimizing the dynamic effort (joint torque square) and maximizing the box weight are the two objective functions. Fourteen human subjects were recruited to collect motion and ground reaction force data in the laboratory. Twelve subjects' data were used to determine cost function weights. The other two subjects' data were used to validate the best MOO objective function weights through the root mean square errors and Pearson coefficients between the simulated and experimental data. The results show that the proposed MOO method and the best weighting coefficients could improve the accuracy of the simulation.

ARTICLE HISTORY

Received 7 June 2019 Accepted 5 December 2019

KEYWORDS

Dynamic effort; maximum lifting weight; dynamic joint strength; inverse dynamics optimization; multi-objective optimization

1. Introduction

Lower back injury during lifting is one of the major musculoskeletal disorders in the workplace. Simulation-based biomechanical models have helped in advancing knowledge of lifting biomechanics and are important tools for assessing injury risks while lifting, as shown in the OpenSim multi-degree-of-freedom musculoskeletal lifting model (Christophy *et al.* 2012) and the Anybody ergonomic lifting model (Stambolian, Eltoukhy, and Asfour 2016). The musculoskeletal model can reveal a great deal of information about muscle force, activation and lumbar spine stress, but it is computationally heavy. In this study, a dynamic-joint-strength-based two-dimensional (2D) skeletal lifting model is developed to evaluate injury risk in the joint space. The skeletal model is used to predict the maximum lifting weight governed by the dynamic joint torque limits, which are functions of joint angle and angular velocity (Xiang *et al.* 2019). The dynamic joint strengths for major joints are obtained from the literature through isometric and isokinetic strength tests (Frey-Law *et al.* 2012; Looft 2014; Hussain and Frey-Law 2016). In this study, the ratio of the joint torque to the dynamic joint strength represents injury risk in the joint space. The proposed skeletal model is computationally efficient and close to real-time implementation.

It is generally difficult to accurately assess a maximum lifting weight through experimental methods because of the risk of injury to human subjects. The traditional US National Institute for Occupational Safety and Health (NIOSH) lifting equation only evaluates a safe lifting weight in the workplace by setting regulated lifting heights, distances and frequencies (Waters, Putz-Anderson,

and Garg 1994). Simulation methods have advantages over traditional experimental methods when predicting the maximum lifting weight, but an accurate subject-specific strength model is required (Hsiang and Ayoub 1994; Khalaf *et al.* 1999; Gündogdu, Anderson, and Parnianpour 2005; Chang *et al.* 2010; Xiang, Arora, *et al.* 2010; Song, Qu, and Chen 2016). It is a challenging task to develop a full-body strength model (Frey-Law *et al.* 2012; Looft 2014; Hussain and Frey-Law 2016). Xiang *et al.* (2019) developed a 2D full-body dynamic joint strength model for symmetrical lifting. This 2D strength model will be used in this study to predict maximum lifting weight.

Multi-objective optimization (MOO) can be applied in everyday fields, such as engineering, economics, automotive, biomechanics, and many others (Marler and Arora 2004; Song, Qu, and Chen 2016; Gunantara and Hendrantoro 2013; Gunantara and Ai 2018). In the biomechanics literature, different optimization methods are used when simulating the lifting motion, such as the computed-muscle-control (CMC) method in OpenSim (Christophy et al. 2012), the forward dynamics optimization method (Huang, Sheth, and Granata 2005), the temporal finite element method (Eriksson and Nordmark 2010) and the inverse dynamics optimization method (Hsiang and Ayoub 1994; Khalaf et al. 1999; Chang et al. 2010; Gündogdu, Anderson, and Parnianpour 2005; Song, Qu, and Chen 2016; Xiang, Arora, et al. 2010; Xiang 2019). These approaches have pros and cons in terms of model complexity, numerical performance, computational reliability and robustness. However, only a few studies have considered MOO for lifting simulation (Xiang, Arora, et al. 2010; Song, Qu, and Chen 2016; Marler, Knake, and Johnson 2011; Ghiasi et al. 2016). Song, Qu, and Chen (2016) presented a MOO method for 2D symmetrical lifting simulation. The two objective functions were minimizing dynamic effort and maximizing load motion smoothness. The results showed that the proposed MOO approach led to accurate predictions compared to the single-objective optimization (SOO) approach. Xiang, Arora, et al. (2010) conducted three-dimensional (3D) skeletal lifting simulation using a MOO approach. The two performance criteria were minimizing dynamic effort and maximizing stability. They concluded from their results that the dynamic effort was a dominating performance measure for lifting motion prediction and the stability criterion played a minor role. The MOO showed robustness for lifting motion prediction and tested different human performance measures (Song, Qu, and Chen 2016; Xiang, Arora, et al. 2010). Marler, Knake, and Johnson (2011) presented lifting posture prediction for a 3D skeletal model with 113 degrees of freedom (DOFs). The two objective functions were minimizing the maximum torque and joint angle. Ghiasi et al. (2016) predicted lumbar spine muscle forces with a given lifting posture and weight using a 3D musculoskeletal model. Two optimization algorithms, vector-evaluated particle swarm optimization (VEPSO) and non-dominated sorting genetic algorithm (NSGA), were employed to solve the optimization problem. The two cost functions were minimizing muscle stress and maximizing the spine stability. It was found that both algorithms predicted consistent muscle activities with the in vivo electromyography data. Although Ghiasi et al. (2016) successfully compared VEPSO and NSGA, the lifting scenario was a fixed posture with given weight. Table 1 summarizes the literature for MOO lifting; none of these studies considered maximum lifting weight as part of the objective function. It is imperative to further explore MOO lifting in the biomedical field.

In the present work, a MOO-based inverse dynamics optimization formulation is developed to predict maximum lifting weight and lifting motion. The MOO problem is solved for the maximum box weight, the corresponding optimal joint angle, joint torque and ground reaction forces (GRF) profiles. Two objective functions are minimized, namely the dynamic effort and negative logarithmic function of the box weight. Dynamic effort is represented as the time integral of the squares of all the joint torques. The negative logarithmic function transforms the box weight maximization problem into a minimization problem. In addition, the predicted box weight range is significantly reduced after applying a logarithmic function on it, which facilitates the normalization process for the weighted sum method of MOO. The hypothesis of this study is that humans try to use an energy-efficient way to lift a maximum weight. Mathematically, this means that box weight is maximized while minimizing an energy-related function. This work is the first study to utilize MOO to predict maximum weight lifting while considering dynamic strength. Real maximum weight cannot be

Table 1. Summary of the literature on multi-objective optimization lifting.

Reference	Motion/posture	Model	Objective functions	Algorithm
Xiang, Arora, et al. (2010)	Motion prediction	3D skeletal with 55 DOFs	Min. torque square + max. stability	SQP
Song, Qu, and Chen (2016)	Motion prediction	2D skeletal with 5 DOFs	Min. torque square + max. motion smoothness	SQP
Ma et al. (2009)	Posture prediction	3D skeletal with 28 DOFs	Min. fatigue + min. discomfort	SQP
Marler, Knake, and Johnson (2011)	Posture prediction	3D skeletal with 113 DOFs	Min. maximum torque + min. joint angle	SQP
Ghiasi et al. (2016)	Given posture with muscle force prediction	3D musculoskeletal lumbar spine with 6 DOFs	Min. muscle stress + max. spine stability	VEPSO and NSGA

Note: 3D = three-dimensional; DOFs = degrees of freedom; SQP = sequential quadratic programming; VEPSO = vector-evaluated particle swarm optimization; NSGA = non-dominated sorting genetic algorithm.

directly measured in experiments; therefore, this study has significance in its ability to predict the subject-specific maximum lifting weight, which can potentially prevent the risk of injury.

2. Methods

2.1. The 2D human model

The 2D model has n = 10 DOFs: three global DOFs (q_1, q_2, q_3) and seven human body joints (q_4, \ldots, q_{10}) , as shown in Figure 1. The global DOFs comprise two translations and one rotation, which move the pelvis to the current position in inertial Cartesian coordinates, while each human body joint is represented by a single rotation in two dimensions. The total DOFs are defined as $\mathbf{q} = [q_1, \ldots, q_{10}]^{\mathrm{T}}$. Besides the spine joint, since the model is symmetrical in the sagittal plane, only one set of shoulder (q_5) , elbow (q_6) , hip (q_7) , knee (q_8) , ankle (q_9) and metatarsophalangeal (q_{10}) joints is modelled in this study. In addition, for these symmetrical joints, the values of joint strength, link mass and moment of inertia are doubled. Recursive Lagrangian dynamics is used to set up the equations of motion for the model (Xiang, Arora, and Abdel-Malek 2009).

Forward recursive kinematics:

$$A_i = A_{i-1}T_i \tag{1}$$

$$\mathbf{B}_{i} = \dot{\mathbf{A}}_{i} = \mathbf{B}_{i-1} \mathbf{T}_{i} + \mathbf{A}_{i-1} \frac{\partial \mathbf{T}_{i}}{\partial q_{i}} \dot{q}_{i}$$
 (2)

$$C_{i} = \dot{\mathbf{B}}_{i} = C_{i-1}\mathbf{T}_{i} + 2\mathbf{B}_{i-1}\frac{\partial \mathbf{T}_{i}}{\partial q_{i}}\dot{q}_{i} + \mathbf{A}_{i-1}\frac{\partial^{2}\mathbf{T}_{i}}{\partial q_{i}^{2}}\dot{q}_{i}^{2} + \mathbf{A}_{i-1}\frac{\partial \mathbf{T}_{i}}{\partial q_{i}}\ddot{q}_{i}$$
(3)

where q_i is the joint angle variable; T_i is the 4×4 Denavit–Hartenberg (DH) link transformation matrix from the (i-1)th link frame to the ith link frame; A_i , B_i and C_i are the global recursive kinematics position, velocity and acceleration matrices, respectively; and $A_0 = [I]$, $B_0 = C_0 = [0]$.

After obtaining all the transformation matrices A_i , B_i and C_i , the global position, velocity and acceleration of a point in Cartesian coordinates can be calculated as

$${}^{\mathrm{o}}\mathbf{r}_{i} = \mathbf{A}_{i}\mathbf{r}_{i}; \ {}^{\mathrm{o}}\dot{\mathbf{r}}_{i} = \mathbf{B}_{i}\mathbf{r}_{i}; \ {}^{\mathrm{o}}\ddot{\mathbf{r}}_{i} = \mathbf{C}_{i}\mathbf{r}_{i}$$

$$\tag{4}$$

where \mathbf{r}_i contains the augmented local coordinates of the point in the *i*th coordinate system.

Backward recursive dynamics:

Each joint torque is defined by Equation (5):

$$\tau_{i} = \operatorname{tr}\left(\frac{\partial A_{i}}{\partial q_{i}}D_{i}\right) - g^{T}\frac{\partial A_{i}}{\partial q_{i}}E_{i} - f_{k}^{T}\frac{\partial A_{i}}{\partial q_{i}}F_{i} - G_{i}^{T}A_{i-1}z_{0}$$
(5)

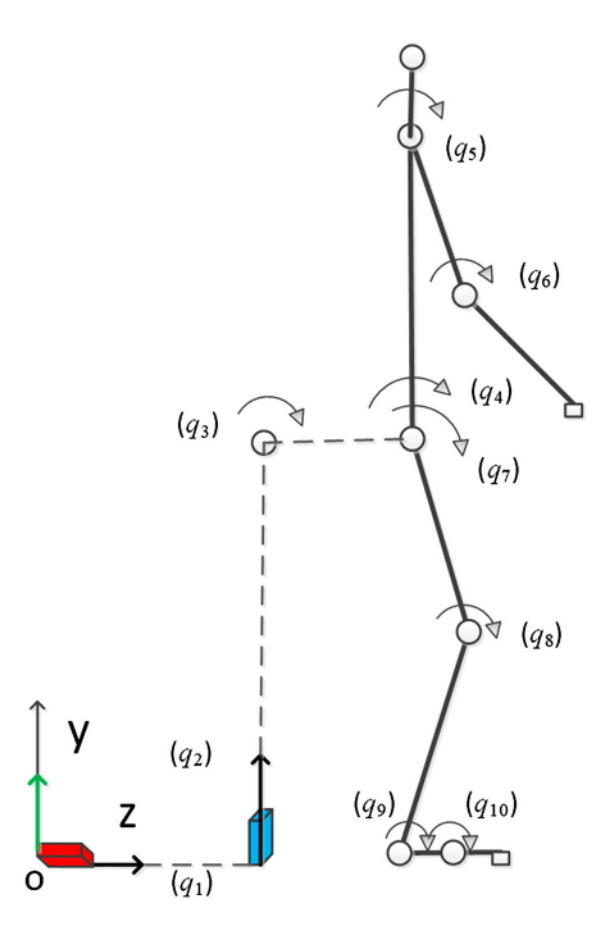


Figure 1. Two-dimensional human model.

$$D_{i} = I_{i}C_{i}^{T} + T_{i+1}D_{i+1}$$
(6)

$$E_i = m_i \mathbf{r}_i + \mathbf{T}_{i+1} E_{i+1} \tag{7}$$

$$\mathbf{F}_i = \mathbf{r}_k \delta_{ik} + \mathbf{T}_{i+1} \mathbf{F}_{i+1} \tag{8}$$

$$G_i = h_k \delta_{ik} + G_{i+1} \tag{9}$$

where $\operatorname{tr}(\cdot)$ is the trace of a matrix; \mathbf{I}_i is the inertia matrix for link i; \mathbf{D}_i is the recursive inertia and Coriolis matrix; \mathbf{E}_i is the recursive vector for gravity torque calculation; \mathbf{F}_i is the recursive vector for external force torque calculation; \mathbf{G}_i is the recursive vector for external moment torque calculation; \mathbf{g} is the gravity vector; m_i is the mass of link i; \mathbf{r}_i is the centre of mass of link i; $\mathbf{f}_k = \begin{bmatrix} 0 & f_{ky} & f_{kz} & 0 \end{bmatrix}^T$ is the external force applied on link k; \mathbf{r}_k is the position of the external force in the local frame k; $\mathbf{h}_k = \begin{bmatrix} h_x & 0 & 0 & 0 \end{bmatrix}^T$ is the external moment applied on link k; $\mathbf{z}_0 = \begin{bmatrix} 0 & 0 & 1 & 0 \end{bmatrix}^T$ is for a revolute joint; $\mathbf{z}_0 = \begin{bmatrix} 0 & 0 & 0 & 0 \end{bmatrix}^T$ is for a prismatic joint; δ_{ik} is Kronecker delta; and the starting conditions are $\mathbf{D}_{n+1} = \mathbf{0}$, $\mathbf{E}_{n+1} = \mathbf{E}_{n+1} = \mathbf{G}_{n+1} = [0]$.

2.2. MOO formulation considering dynamic strength

For the optimization problem, the time domain is discretized using cubic B-spline functions. Thus, a joint angle profile q(t) is parameterized as follows:

$$q_i(t, \mathbf{s}, \mathbf{P}_i) = \sum_{i=0}^{m} N_j(t, \mathbf{s}) P_{ij}; \quad 0 \le t \le T$$
 (10)

where t is the time instant; $N_i(t, s)$ are the basis functions; s is the knot vector; and $P_{ii} = \{p_{i0}, \dots, p_{im}\}$ is the control points vector for the *i*th joint angle profile and m+1 is the number of control points. The shape of the joint angle profile can thus be affected by changing the value of the control points. With this representation, the control points become the optimization variables. In this study, the box weight (W) is also the design variable, and the knot vector is specified and fixed in the optimization process. Five control points are used for each DOF. Thus, there is a total of $5 \times n + 1(W) = 51$ optimization variables $\mathbf{x} = \begin{bmatrix} \mathbf{P}_1^T & \cdots & \mathbf{P}_n^T & \mathbf{W} \end{bmatrix}^T$ in the formulation. Then, the joint angular velocity $(\dot{\mathbf{q}})$ and acceleration (q) can be obtained from the first and second time derivatives of the B-spline discretization of the joint angle profile, respectively. Therefore, all joint state variables (q, \dot{q}, \ddot{q}) are functions of B-spline control points (P). Next, based on the joint state variables, the DH-based forward recursive kinematics (Equation 4) is calculated for points of interest in the human model (foot or foot and hand $^{\circ}$ r_{hand}). In addition, the joint torque $\tau(x)$ is computed by plugging the joint state variables and box weight (external load) directly into equations of motion (Equation 5), and this is the inverse dynamics procedure. The lifting task is formulated as a general nonlinear programming problem: find the optimal design variables x to minimize a human performance measurement, f(x), subject to physical constraints, as follows:

Find: **x**
To
$$\min f(\mathbf{x})$$
S.t. $h_i = 0, \quad i = 1, ..., l$
 $g_j \le 0, \quad j = 1, ..., k$
(11)

where h_i are the equality constraints and g_j are the inequality constraints. Expressions for f, h_i and g_j are given in the following paragraphs.

A new multi-objective function (f) is introduced in this study to minimize the joint torque square and negative logarithmic function of box weight simultaneously:

$$f = w_1 N \left[\int_0^T \sum_{i=4}^n \left(\frac{\tau_i(\mathbf{x}, t)}{\tau_i^U - \tau_i^L} \right)^2 dt \right] - w_2 N[\log(W + 10)]$$
 (12)

where N[·] is the normalization function; τ_i^L and τ_i^U are the *i*th lower and upper dynamic joint torque limits, respectively (Xiang *et al.* 2019); T is the total box lifting time; and w_1 and w_2 are weighting coefficients for the two normalized objective functions, where $w_1 + w_2 = 1$.

The lifting optimization problem is subject to the following constraints: first, joint angle limits:

$$\mathbf{q}^L < \mathbf{q}(\mathbf{x}, t) < \mathbf{q}^U \tag{13}$$

where \mathbf{q}^L and \mathbf{q}^U are the lower and upper joint angle bounds.

Dynamic strength is considered in the simulation and imposed as joint torque limits:

$$\tau_i^L(q_i, \dot{q}_i, z_{\text{score}}, t) \le \tau_i(\mathbf{x}, t) \le \tau_i^U(q_i, \dot{q}_i, z_{\text{score}}, t); \quad i = 4, ..., 10$$
 (14)

where the lower and upper torque limits are functions of joint angle (q), angular velocity (\dot{q}) , strength percentile (z_{score}) and time (t): $\tau_i^L = \tau_i^L(q_i, \dot{q}_i, z_{\text{score}}, t)$, $\tau_i^U = \tau_i^U(q_i, \dot{q}_i, z_{\text{score}}, t)$; these two functions are regression equations obtained from isometric and isokinetic strength tests using dynamometers (Xiang *et al.* 2019; Frey-Law *et al.* 2012; Looft 2014; Hussain and Frey-Law 2016).

Balance must be considered during the box lifting process. This is the zero moment point (ZMP) constraint,

$${}^{o}\mathbf{r}_{ZMP}(\mathbf{x}, t) \in FSR$$
 (15)

where ${}^{\circ}r_{ZMP}$ is the calculated ZMP location (Xiang, Arora, et al. 2010); and FSR is the foot support region.



In addition, feet are fixed on level ground:

$${}^{o}\mathbf{r}_{\text{foot}}(\mathbf{x}, t) = {}^{o}\mathbf{r}_{\text{foot}}^{E} \tag{16}$$

where or foot is the calculated global foot position from the 2D human model using Equation (4); and ${}^{o}\mathbf{r}_{\text{foot}}^{E}$ is the measured foot position from the experiment.

The initial and final box grasping locations are given based on experimental data:

$${}^{\mathrm{o}}\mathbf{r}_{\mathrm{hand}}(\mathbf{x}, t) = {}^{\mathrm{o}}\mathbf{r}_{\mathrm{box}}^{E}(t); \quad t = 0, T$$

$$\tag{17}$$

where ${}^{o}\mathbf{r}_{hand}$ is the calculated global hand position using Equation (4); and ${}^{o}\mathbf{r}_{hox}^{E}$ is the measured box handle position from experiments.

Finally, the boundary and mid-time joint angle differences between the model and experiments are constrained in a small range $\varepsilon=0.1$ rad at the boundary and $\varepsilon=0.15$ rad at mid-time, where q_i^E is the experimental joint angle for the ith physical joint:

$$|q_i(\mathbf{x}, t) - q_i^E(t)| \le \varepsilon; \quad i = 4, ..., 10; \quad t = 0, \frac{T}{2}, T$$
 (18)

The time-dependent constraints in Equations (13)-(16) are evaluated not only at the knot timepoint, but also at two additional time-points between any two adjacent distinguished knots. The timeindependent constraints in Equations (17) and (18) are evaluated only at the given specific timepoints. There is a total of 295 nonlinear constraints for the MOO lifting problem. The bounds for the design variables x are: $P_{ij} \in [-10, 10]$ rad and $W \in [0, 1000]$ N. The initial guesses are: P = 0 and W = 200. The computation is close to real time.

2.3. Experimental data collection

2.3.1. Participants

Twenty-three male subjects aged 20-50 years participated in the laboratory experiments; among them, four subjects' motion data were found to be incomplete during the data postprocessing stage and were therefore discarded. Among the remaining 19, 14 subjects were using a squat lifting strategy (gender: male; age: 25.50 ± 7.22 years; height: 180.64 ± 5.15 cm; body mass: 82.34 ± 10.45 kg, where \pm indicates standard deviation). Therefore, these 14 subjects were used for this study: 12 subjects for MOO simulation and two subjects for MOO validation. The recruitment criteria were that subjects should be physically and mentally sound, able to perform the scripted task and not be on any medication that might hamper their performance in the box lifting task. The experimental protocol was approved by the Institutional Review Board of Texas Tech University and all subjects signed the consent form.

2.3.2. Experimental protocol

A Vicon Nexus motion-capture system with five cameras (VICON, Oxford, UK) was used to collect kinematic data at 100 Hz. A plug-in-gait model with added iliac crests, giving 42 markers in total, was used for the marker protocol (Cloutier, Boothby, and Yang 2011). Two Kistler force plates (Kistler, Winterthur, Switzerland) were used to collect GRFs at 2000 Hz and each foot was placed on one of the force plates. For each subject, the following anthropometrics were measured: height, weight, leg length, ankle width, knee width, wrist width, elbow width, shoulder offset, inter-anterior superior iliac spine (inter-ASIS) distance and waist circumference (Mital and Kromodihardjo 1986; Schultz et al. 1982).

During the experiment, each participant was asked to psychophysically test their maximum weight lifting capability by gradually adding the load until the subject requested that the increase be stopped.



Figure 2. Box-lifting experiment.

The real maximum weight lifting capacity was not adopted to avoid any injury during the experiment, i.e. the maximum weight in this study refers to the maximum weight that the participant could lift safely. Once the maximum lifting weight had been obtained, the participant was ready to perform the lifting task. The subject was requested to lift a box (65 cm \times 35 cm \times 15 cm) forward, i.e. symmetrical lifting, in three trials. Because the box did not have handles, it was placed on top of a weight disc, measuring about 2.54 cm high, on the floor, so that the subject could fit his fingers under the box. The subject then lifted the box in the most comfortable and natural way and set it down on a 1 m tall table in front of them, as shown in Figure 2. After data collection, the data postprocessing was conducted in the motion capture software Vicon Nexus.

2.3.3. Data processing

The first step for data postprocessing was marker labelling. Then, the data were smoothed and converted into a C3D file. Finally, the C3D file was imported into Visual 3D (C-Motion, Germantown, MD, USA). Within Visual 3D, a skeletal model with 15 segments based on the marker protocol used in the experiments was created to output coordinates and joint angles. The anthropometric measurements taken for each subject at the beginning of the experiment were used to create distinct and accurate skeletal models, allowing for more precise calculations.

The measured height and body mass for each subject at the beginning of the experiment were used to generate their body segments' lengths, centres of mass and inertial properties using GEBODTM, a regression-based interactive utility (Cheng, Obergefell, and Rizer 1994). Six joint angles (spine, shoulder, elbow, hip, knee and ankle), the box weight obtained from the experiments for each individual subject and the generated anthropometrics were used to obtain the strength percentile (z_{score}) for each subject (Xiang et al. 2019). Finally, the proposed 2D symmetrical MOO inverse dynamics motion simulation was used to predict motions, GRF and maximum box weights. Note that the MOO algorithm in this study is an in-house program developed in MATLAB.

2.4. Total error for MOO weighting coefficients

In Section 2.2, two weighting coefficients are defined, where $w_1 + w_2 = 1$. For each subject, 21 Pareto cases (0-20) are established, where the first case has $w_1 = 0.0$ for dynamic effort and $w_2 = 1.0$ for box weight. The remaining cases are created by increasing w_1 by 0.05 and decreasing w_2 by 0.05 until the final case set $w_1 = 1.0$ and $w_2 = 0.0$. A Pareto-optimal analysis, in conjunction with the total error (E_{Total}) analysis, is performed to determine the best case (weighting coefficients) for each subject. The experimental joint angle profiles, GRF profiles and box weight are compared to the simulation data for all 21 cases. In this study, the total error for each case is defined as

$$E_{\text{Total}} = \frac{RMSE_q}{RMSE_{qmax}} + \frac{RMSE_{vGRF}}{RMSE_{vGRFmax}} + \frac{RMSE_{hGRF}}{RMSE_{hGRFmax}} + \frac{E_W}{E_{Wmax}}$$
(19)

where RMSE_a is the total root mean square error (RMSE) for the six major joint angle profiles (spine, shoulder, elbow, hip, knee and ankle); RMSE_{vGRF} is the total RMSE for the vertical GRF profile; $RMSE_{hGRF}$ is the total RMSE for the horizontal GRF profile; and E_W is the error for the box weight prediction. Note that joint angle and GRF profiles are vectors and box weight is a scalar. The total error E_{Total} is normalized by dividing each error by its respective maximum error found among the 21 cases for that specific subject. After identifying the total error for all cases for each of the 12 subjects, an average total error is calculated for each case across all subjects. The Pareto case with the lowest average total error is chosen as the optimal values for the two weighting coefficients.

2.5. Validation

After identifying the best MOO weighting coefficients for the lifting model through total error analysis, the other two experimental subjects are compared to their respective simulation results with and without MOO. The error of the predicted box weight and RMSE of each individual joint, vertical GRF and horizontal GRF profiles are calculated. In addition, Pearson coefficients for each individual joint and GRF profiles are calculated.

3. Results

3.1. Maximum weight lifting MOO for 12 subjects

As mentioned in Section 2.2, both objective functions are appropriately normalized so that they have the same absolute magnitudes in the range [0, 1]. The MOO problem is depicted in the criterion space where the two axes represent two objective functions as shown in Figure 3. For example, the normalized joint torque square and normalized negative logarithmic function of box weight are plotted for Subject 3. The Pareto-optimal curve is plotted in the criterion space by evaluating the objective functions for 21 cases in Equation (12) by systematically varying weighting coefficients. The dots represent the Pareto-optimal solution for each case. Similarly, for the other subjects, Pareto-optimal curves are plotted by evaluating the objective functions for 21 cases in the criterion space as shown in Figure 3.

3.2. Best MOO weighting coefficients for maximum weight lifting

After calculation of the average total error for all Pareto cases of the 12 subjects, Pareto case 3, where $w_1 = 0.15$ and $w_2 = 0.85$, has the lowest average total error, with a value of 2.621. Pareto case 20 has the highest average total error of 3.337. As shown in Figure 4, the further away from case 3, the higher the average total error value. Next, the maximum weight lifting motions of Subjects 2 and 9 are simulated using the proposed MOO approach with the best weighting coefficients obtained from the 12 subjects' simulation pool. The results of MOO are compared with the simulation using a single maximum weight objective function. The RMSE and Pearson coefficients for simulation with MOO

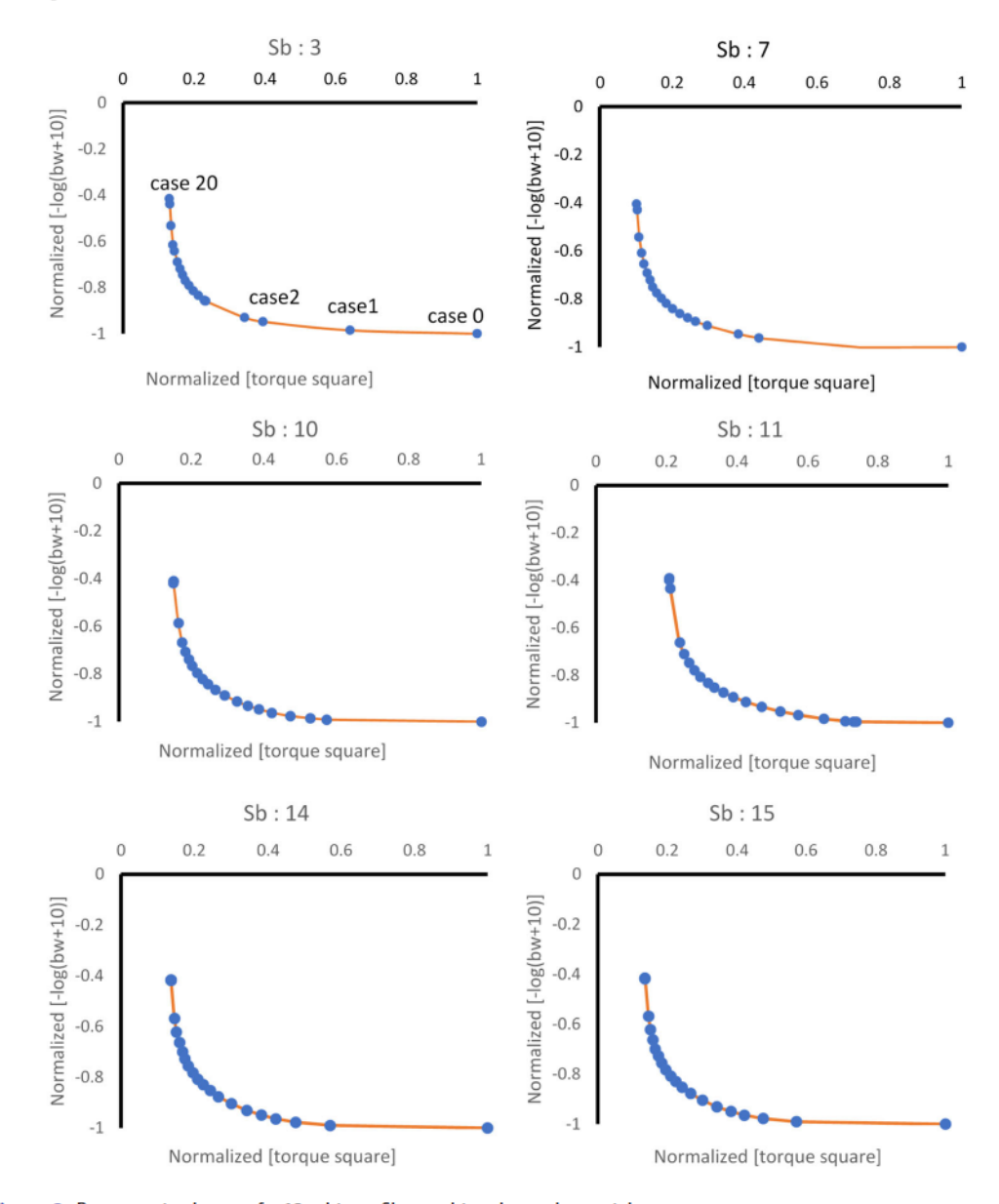


Figure 3. Pareto-optimal curves for 12 subjects. Sb = subject; bw = box weight.

and without MOO are presented in Tables 2 and 3, respectively. A visual comparison between the experimental data and their respective simulations can be seen in Figures 5 and 6.

4. Discussion and conclusions

The basic idea of the proposed MOO is to maximize the box weight while minimizing an energy-related function, *i.e.* joint torque square. The weighted sum method of MOO is used to aggregate the two objective functions. The lifting motions of the 12 subjects are simulated and each one has 21 cases, making a total of $12 \times 21 = 252$ simulations. Next, the overall average total error for each case is calculated across the 12 subjects and the case with the minimal error gives the best Pareto-optimal weighting coefficients. In this study, the identified best weighting coefficients are 0.15 for dynamic

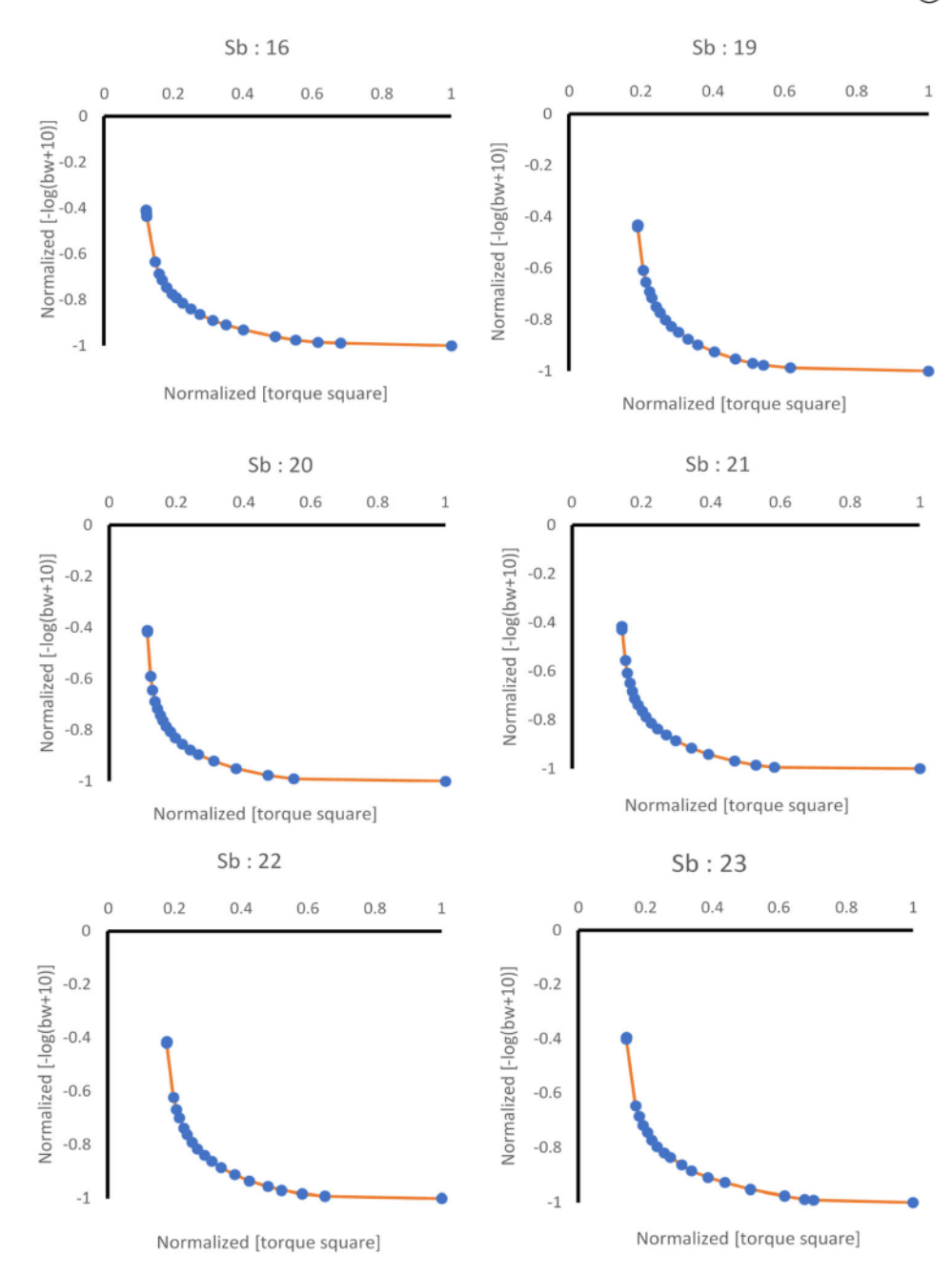


Figure 3. Continued.

effort and 0.85 for box weight, as shown in Figure 4. It is seen that the box weight has a larger effect than the dynamic effort objective function; this is quite reasonable because the goal of the simulation is to maximize the lifting weight.

In Figure 3, the smooth Pareto-optimal curves are generated for all 12 subjects. These smooth curves indicate that the numerical performance is stable for the proposed MOO approach. It is noted that the Pareto-optimal solutions between case 0 (0.0, 1.0) and case 2 (0.1, 0.9) are almost on a horizontal straight line, where the dynamic effort changes substantially but the box weight remains almost

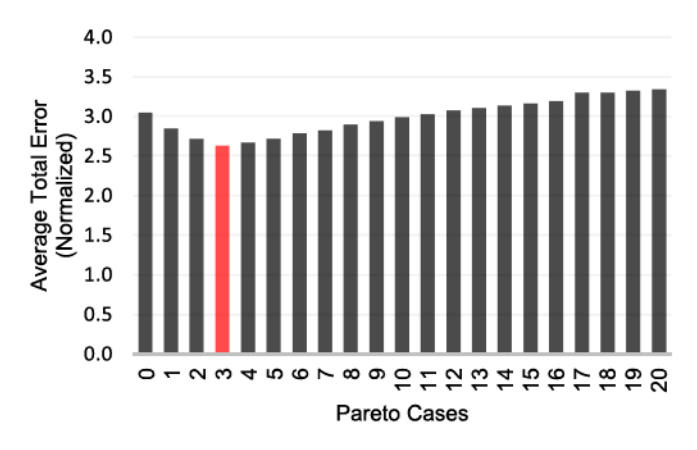


Figure 4. Average total error (normalized) for each Pareto case.

Table 2. Error results for simulation with multi-objective optimization (MOO) and without MOO.

	Subject 2		Subject 9	
	With MOO	Without MOO	With MOO	Without MOO
RMSE spine	11.497	17.268	7.900	12.616
RMSE shoulder	10.424	10.143	16.025	11.176
RMSE elbow	7.167	13.039	8.395	20.572
RMSE hip	6.276	7.600	5.050	4.700
RMSE knee	9.743	7.254	6.705	8.221
RMSE ankle	8.244	2.703	7.652	2.691
RMSE Q	53.350	58.007	51.727	59.976
RMSE vertical GRF	121.864	122.050	71.542	68.891
RMSE horizontal GRF	48.976	59.470	57.580	53.900
Error W	8.536	24.303	19.563	20.429

Note: RMSE Q = root mean square error sum of spine, shoulder, elbow, hip, knee and ankle joints; GRF = ground reaction force; W = weight.

Table 3. Pearson coefficient (r value) results for simulation with multi-objective optimization (MOO) and without MOO.

	Subject 2		Subject 9	
	With MOO	Without MOO	With MOO	Without MOO
Spine	0.928	0.593	0.997	0.708
Shoulder	0.980	0.957	0.956	0.865
Elbow	0.986	0.709	0.994	0.780
Hip	0.990	0.989	0.994	0.994
Knee	0.988	0.995	0.998	0.994
Ankle	0.914	0.990	0.910	0.994
Vertical GRF	0.334	0.268	0.712	0.674

Note: GRF = ground reaction force.

at a constant value (maximum). Similarly, the optimal solutions between case 20 (1.0, 0.0) and case 18 (0.9, 0.1) are located on a steep vertical line, where the box weight changes substantially but the dynamic effort does not change much. The Pareto-optimal curve represents the trade-off between the two objectives. For the maximum weight lifting simulation, it is advantageous to choose cases close to the horizontal flat portion of the Pareto-optimal curve, where the maximum box weight is achieved with less dynamic effort. For example, relative to case 2, case 1 represents a substantial increase in effort for just a small improvement in box weight. Thus, case 2 is preferred over case 1 (Xiang, Arora, et al. 2010; Marler and Arora 2004; Gunantara and Ai 2018). Note that w = (0.15, 0.85) corresponding to case 3 is identified as the best weighting coefficients to aggregate two objective functions.

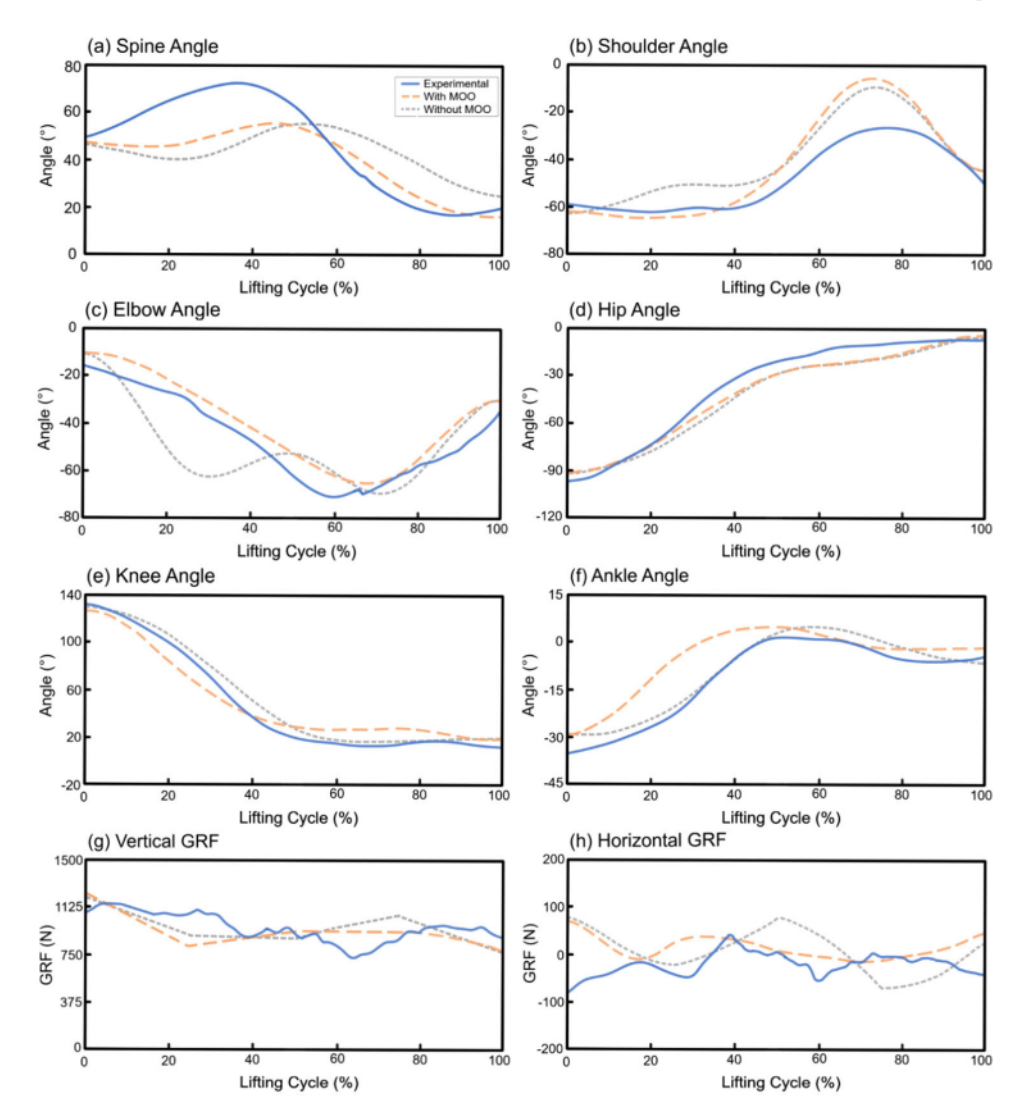


Figure 5. Joint angle and ground reaction force (GRF) profiles validation for subject 2.

The suggested weighting coefficients (0.15, 0.85) from the pool of 12 subjects is used to simulate the maximum weight lifting motions for the other two subjects: Subjects 2 and 9. Table 2 shows that both subjects have smaller RMSE Q values (total kinematics error) with MOO than those without MOO. Similarly, for the predicted box weight, MOO gives a smaller error than the simulation without MOO. For GRFs, Subject 2 has a smaller error using the MOO method; however, for Subject 9, MOO generates a relatively large error. This may be due to the inaccuracy of the GRF simulation in the model, e.g. the initial lifting acceleration that exists in experiments is not incorporated in the optimization formulation in Section 2.2. Based on the results from Table 2, this demonstrates that using MOO generally results in smaller simulation errors.

The Pearson coefficient results show that using MOO gives a stronger correlation between simulation and experiment than without MOO. For Subject 2, the r values are larger using MOO, except for the knee and ankle joints. For Subject 9, the r values are larger using MOO, except for the ankle joint. The Pearson coefficients (r values) show that the proposed MOO is an effective approach for simulating maximum weight lifting motion compared to the SOO approach.

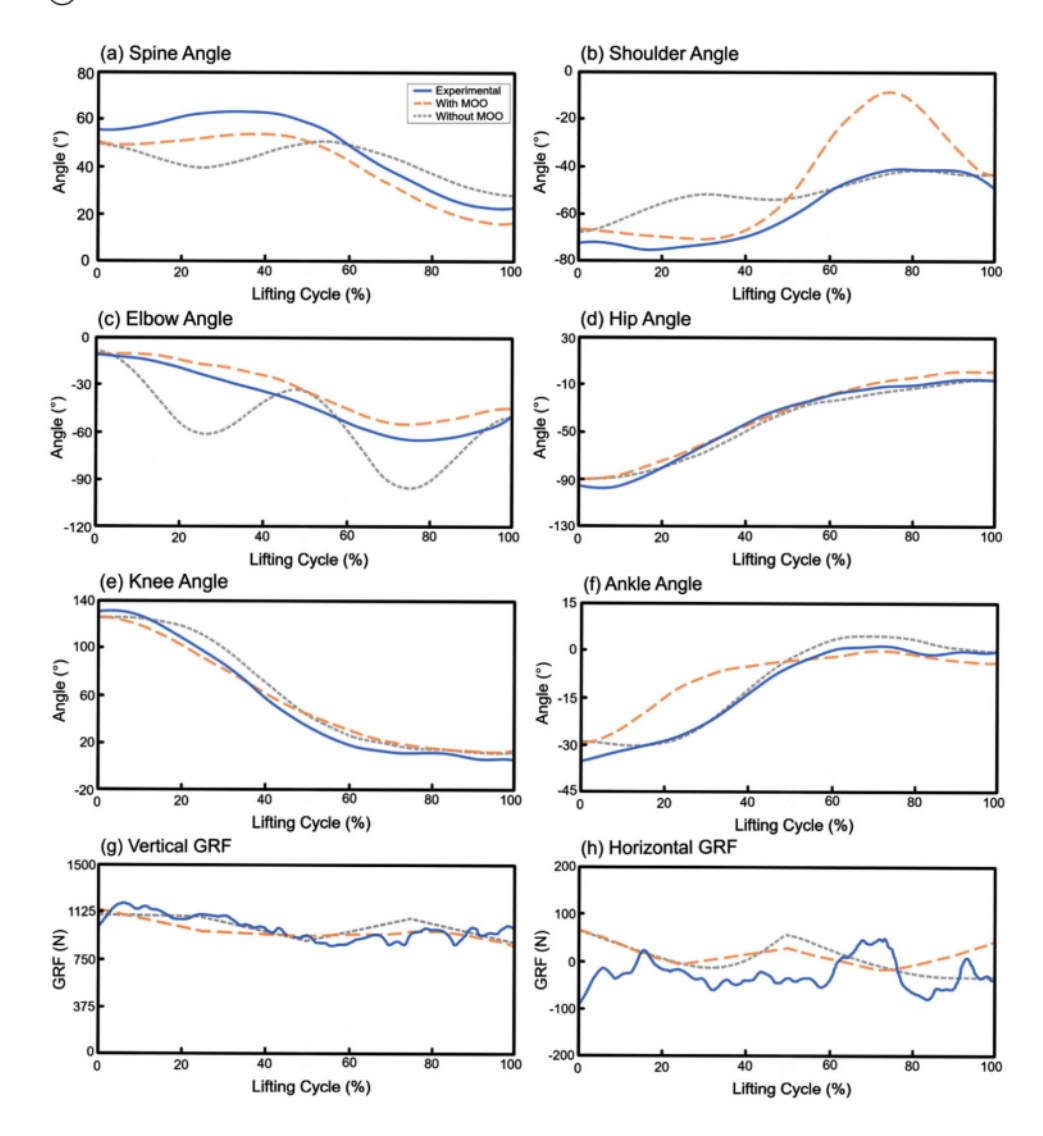


Figure 6. Joint angle and ground reaction force (GRF) profiles validation for subject 9.

Figures 5 and 6 compare the joint angle and GRF profiles for Subjects 2 and 9 between simulation and experiment. For Subject 2 (Figure 5), it is apparent that using MOO gives more accurate simulation results than without using MOO, except for the ankle joint. For Subject 9 (Figure 6), MOO generates better simulations for spine, elbow, hip and knee joints. Overall, MOO has a smaller total kinematics RMSE value, as seen in Table 2 (RMSE Q).

There are some limitations to this study. First, only 2D symmetrical lifting motion is simulated. Secondly, there are potential inaccuracies in the dynamic joint strength database from the literature. Thirdly, three postures from the experiments are imposed as constraints in Equation (18), at the initial time, mid-time and final time. Based on the authors' previous study (Xiang, Chung, *et al.* 2010), these experimental constraints are necessary to produce more accurate simulations for complicated whole-body lifting motions.

This study presents a MOO method that predicts a subject-specific maximum lifting weight and lifting motion while considering the subject's dynamic strength. This prediction is achieved using aggregated objective functions and identified weighting coefficients for maximum weight lifting

simulation. It has been demonstrated that the MOO approach generates more accurate simulations compared to the cases without MOO. The hypothesis that humans are using energy-efficient ways to lift the maximum weight has been proven. Future work includes: (1) extending the 2D model to a 3D lifting simulation using a MOO approach; (2) extending the skeletal model to a musculoskeletal model; and (3) conducting a lumbar spine injury study using the proposed MOO approach and musculoskeletal model.

Disclosure statement

No potential conflict of interest was reported by the authors.

Funding

This work is supported by the National Science Foundation [CBET: 1849279 and 1703093].

References

Chang, C. C., R. W. McGorry, J. H. Lin, X. Xu, and S. M. Hsiang. 2010. "Prediction Accuracy in Estimating Joint Angle Trajectories Using a Video Posture Coding Method for Sagittal Lifting Tasks." Ergonomics 53 (8): 1039–1047.

Cheng, H., L. Obergefell, and A. Rizer. 1994. Generator of Body Data (GEBOD) Manual. Dayton, OH, USA.

Christophy, M., N. A. F. Senan, J. C. Lotz, and O. M. O'Reilly. 2012. "A Musculoskeletal Model for the Lumbar Spine." Biomechanics and Modeling in Mechanobiology 11 (1/2): 19–34.

Cloutier, A., R. Boothby, and J. Yang. 2011. "Motion Capture Experiments for Validating Optimization-Based Human Models." HCI International, 3rd International Conference on Digital Human Modelling, July 9–14, Florida, USA.

Eriksson, A., and A. Nordmark. 2010. "Temporal Finite Element Formulation of Optimal Control in Mechanisms." Computer Methods in Applied Mechanics and Engineering 199: 1783–1792.

Frey-Law, L. A., A. Laake, K. G. Avin, J. Heitsman, T. Marler, and K. Abdel-Malek. 2012. "Knee and Elbow 3D Strength Surfaces: Peak Torque-Angle-Velocity Relationships." *Journal of Applied Biomechanics* 28 (6): 726–737.

Ghiasi, M. S., N. Arjmand, M. Boroushaki, and F. Farahmand. 2016. "Investigation of Trunk Muscle Activities During Lifting Using a Multi-objective Optimization-Based Model and Intelligent Optimization Algorithms." *Medical & Biological Engineering & Computing* 54: 431–440.

Gunantara, N., and Ai, Q. 2018. "A Review of Multi-objective Optimization: Methods and Its Applications." Cogent Engineering 5 (1): 1502242.

Gunantara, N., and G. Hendrantoro. 2013. "Multi-objective Cross-Layer Optimization for Selection of Cooperative Path Pairs in Multihop Wireless Ad Hoc Networks." *Journal of Communications Software and Systems* 9 (3): 170–177.

Gündogdu, Ö, K. S. Anderson, and M. Parnianpour. 2005. "Simulation of Manual Materials Handling: Biomechanical Assessment Under Different Lifting Conditions." *Technology and Health Care* 13 (1): 57–66.

Hsiang, S. M., and M. M. Ayoub. 1994. "Development of Methodology in Biomechanical Simulation of Manual Lifting." International Journal of Industrial Ergonomics 13: 271–288.

Huang, C., P. N. Sheth, and K. P. Granata. 2005. "Multibody Dynamics Integrated with Muscle Models and Space-Time Constraints for Optimization of Lifting Movements." ASME International Design Engineering Technical Conferences, September 24–28, Long Beach, CA, USA.

Hussain, S. J., and L. A. Frey-Law. 2016. "3D Strength Surfaces for Ankle Plantar- and Dorsi-flexion in Healthy Adults: An Isometric and Isokinetic Dynamometry Study." *Journal of Foot and Ankle Research* 9 (43): 1–10.

Khalaf, K. A., M. Parnianpour, P. J. Sparto, and K. Barin. 1999. "Determination of the Effect of Lift Characteristics on Dynamic Performance Profiles During Manual Materials Handling Tasks." *Ergonomics* 42 (1): 126–145.

Looft, J. M. 2014. "Adaptation and Validation of an Analytical Localized Muscle Fatigue Model for Workplace Tasks." Ph.D. thesis, Department of Biomedical Engineering, The University of Iowa, Iowa City, IA, USA.

Ma, L., W. Zhang, D. Chablat, F. Bennis, and F. Guillaume. 2009. "Multi-objective Optimization Method for Posture Prediction and Analysis with Consideration of Fatigue Effect and Its Application Case." Computers & Industrial Engineering 57 (4): 1235–1246.

Marler, T., and J. S. Arora. 2004. "Survey of Multi-objective Optimization Methods for Engineering." Structural and Multidisciplinary Optimization 26 (6): 369–395.

Marler, T., L. Knake, and R. Johnson. 2011. "Optimization-Based Posture Prediction for Analysis of Box Lifting Tasks." In Digital Human Modeling, edited by V. G. Duffy, 151–160. Berlin: Springer.

Mital, A., and S. Kromodihardjo. 1986. "Kinetic Analysis of Manual Lifting Activities: Part II -Biomechanical Analysis of Task Variables." *International Journal of Industrial Ergonomics* 1: 91–101.

Schultz, A. B., B. J. Anderson, K. Haderspeck, R. Ortexgren, M. Nordin, and R. Bjork. 1982. "Analysis and Measurement of Lumber Trunk Loads in Tasks Involving Bends and Twists." *Journal of Biomechanics* 15 (9): 669–675.



- Song, J., X. Qu, and C. H. Chen. 2016. "Simulation of Lifting Motions Using a Novel Multi-objective Optimization Approach." International Journal of Industrial Ergonomics 53: 37-47.
- Stambolian, D., M. Eltoukhy, and S. Asfour. 2016. "Development and Validation of a Three Dimensional Dynamic Biomechanical Lifting Model for Lower Back Evaluation for Careful Box Placement." International Journal of Industrial Ergonomics 54: 10-18.
- Waters, T., V. Putz-Anderson, and A. Garg. 1994. Applications Manual for the Revised NIOSH Lifting Equation. DHHS (NIOSH) Publication No. 94-110, Cincinnati, OH, USA.
- Xiang, Y. 2019. "An Inverse Dynamics Optimization Formulation with Recursive B-Spline Derivatives and Partition of Unity Contacts: Demonstration Using Two-Dimensional Musculoskeletal Arm and Gait." Journal of Biomechanical Engineering 141 (3): 034503.
- Xiang, Y., J. S. Arora, and K. Abdel-Malek. 2009. "Optimization-Based Motion Prediction of Mechanical Systems: Sensitivity Analysis." Structural and Multidisciplinary Optimization 37 (6): 595-608.
- Xiang, Y., J. S. Arora, S. Rahmatalla, T. Marler, R. Bhatt, and K. Abdel-Malek. 2010. "Human Lifting Simulation Using a Multi-objective Optimization Approach." Multibody System Dynamics 23 (4): 431-451.
- Xiang, Y., H. J. Chung, J. H. Kim, R. Bhatt, S. Rahmatalla, J. Yang, T. Marler, J. S. Arora, and K. Abdel-Malek. 2010. "Predictive Dynamics: An Optimization-Based Novel Approach for Human Motion Simulation." Structural and Multidisciplinary Optimization 41: 465-479.
- Xiang, Y., R. Zaman, R. Rakshit, and J. Yang. 2019. "Subject-Specific Strength Percentile Determination for Two-Dimensional Symmetric Lifting Considering Dynamic Joint Strength." Multibody System Dynamics 46 (1): 63-76.